hexafluorophosphate in ACN/MC (1:5 by volume). The electropolymerization for electrochemical study was carried out at a monomer concentration of 2 mM. The electrochemical cells were deaerated by nitrogen bubbling prior to each experiment. The setup for the spectroelectrochemical measurements was described in a previous publication [13]. Glass coated with indium tin oxide (100 $\Omega\,\square^{-1}$, Delta-Technology Inc., active diameter 10 mm) was used as a working electrode for spectroelectrochemical measurements. In the static electrochromic experiment, spectra were obtained after the current decayed to almost zero at the given potential. In the dynamic electrochromic experiment, the changes in current and absorbance at 610 nm were monitored simultaneously during a square wave potential step with 40 s period.

Received: February 17, 2004
Final version: June 5, 2004

[1] P. M. S. Monk, R. J. Mortimer, D. R. Rosseinsky, *Electrochromism: Fundamentals and Applications*, VCH, Weinheim, Germany **1995**.
[2] G. Heywang, F. Jonas, *Adv. Mater.* **1992**, *4*, 116.
[3] a) M. Dietrich, J. Heinze, G. Heywang, F. Jonas, *J. Electroanal. Chem.* **1994**, *369*, 87. b) L. Groenendaal, G. Zotti, P.-H. Aubert, S. M. Waybright, J. R. Reynolds, *Adv. Mater*. **2003**, *15*, 855.
[4] a) L. Groenendaal, G. Zotti, F. Jonas, *Synth. Met.* **2001**, *118*, 105. b) K. Krishnamoorthy, M. Kanungo, A. Q. Contractor, A. Kumar, *Synth. Met.* **2001**, *124*, 471. c) I. Schwendeman, C. L. Gaupp, J. M. Hancock, L. Groenendaal, J. R. Reynolds, *Adv. Funct. Mater.* **2003**, *13*, 541.
[5] a) A. Kumar, D. M. Welsh, M. C. Morvant, F. Piroux, K. A. Abboud, J. R. Reynolds, *Chem. Mater.* **1998**, *10*, 896. b) D. M. Welsh, A. Kumar, E. W. Meijer, J. R. Reynolds, *Adv. Mater.* **1999**, *11*, 1379. c) K. Krishnamoorthy, A. V. Ambade, M. Kanungo, A. Q. Contractor, A. Kumar, *J. Mater. Chem.* **2001**, *11*, 2909. d) C. L. Gaupp, D. M. Welsh, J. R. Reynolds, *Macromol. Rapid Commun.* **2002**, *23*, 885. e) A. Cirpan, A. A. Argun, C. R. G. Grenier, B. D. Reeves, J. R. Reynolds, *J. Mater. Chem.* **2003**, *13*, 2422.
[6] P. M. S. Monk, *The Viologens: Physicochemical Properties, Synthesis and Applications of the Salts of 4,4′-Bipyridine*, Wiley, New York **1998**.
[7] D. M. DeLongchamp, M. Kastantin, P. T. Hammond, *Chem. Mater.* **2003**, *15*, 1575.
[8] S. C. Ng, H. S. O. Chan, W.-L. Yu, *J. Mater. Sci. Lett.* **1997**, *16*, 809.
[9] A. Kros, R. J. M. Nolte, N. A. J. M. Sommerdijk, *J. Polym. Sci., Part A: Polym. Chem.* **2002**, *40*, 738.
[10] M. Lapkowski, A. Pron, *Synth. Met*. **2000**, *110*, 79.
[11] S. A. Sapp, G. A. Sotzing, J. R. Reynolds, *Chem. Mater.* **1998**, *10*, 2101.
[12] A. Lima, P. Schottland, S. Sadki, C. Chevrot, *Synth. Met.* **1998**, *93*, 33. Careful spectroscopic study showed the procedure yielded the desired product along with 3,4-dihydro-2*H*-thieno[3,4-*b*][1,4]dioxepin-3-methanol in 4:1 ratio. Since this monomer was inseparable from the desired product and expected to show similar properties to (2,3-dihydrothieno[3,4-*b*]-[1,4]dioxin-2-yl)methanol, the whole synthesis was carried out as a mixture with this minor component.
[13] H. C. Ko, S. Park, W. Paik, H. Lee, *Synth. Met.* **2002**, *132*, 15.

Organic Nanostructured Host–Guest Materials Containing Three Dyes**

By *Chiara Botta*,* *Greta Patrinoiu*, *Pierre Picouet*,
Sami Yunus, *Jean-Edouard Communal*,
Fabrizio Cordella, *Francesco Quochi*, *Andrea Mura*,
Giovanni Bongiovanni, *Mariacecilia Pasini*,
Silvia Destri, and *Giuseppe Di Silvestro*

Stable materials that absorb light at short wavelengths and efficiently emit photons at lower energies provide low-cost solutions for tuning the color of light-emitting diodes across the entire visible spectrum, and for sensitizing photovoltaic cells or silicon detectors.[1] Due to the ability of perhydrotriphenylene (PHTP) to form inclusion compounds (ICs),[2] the inclusion of linear conjugated dyes in PHTP represents a novel method for obtaining organic host–guest materials that are able to funnel the excitation to a desired site, and to perform the specific function of efficient photon down-conversion. In such materials, the supramolecular organization imposes an *optimal* lateral distance between the active molecules of 1.4 nm, which is short enough to obtain both high dye concentrations and efficient long-range energy transfer (ET), but long enough to avoid concentration quenching of luminescence.[3]

PHTP-based host–guest materials with emissive molecules have been obtained for both oligothiophene[2,4] and oligo(phenylene vinylene)[5] derivatives. Recently, we have shown that PHTP co-inclusion compounds (co-ICs), obtained by the inclusion of two dyes possessing the appropriate optical properties, provide systems that, thanks to the optimal dye orienta-

---

[*] Dr. C. Botta, Dr. G. Patrinoiu, Dr. P. Picouet, Dr. S. Yunus, Dr. M. Pasini, Dr. S. Destri
Istituto per lo Studio delle Macromolecole, CNR
via E. Bassini 15, I-20133 Milano (Italy)
E-mail: chiara.botta@ismac.cnr.it

Dr. G. Patrinoiu
"I. G. Murgulescu" Institute of Physical Chemistry
Spl. Independentei 202, RO-77208 Bucharest (Romania)

Dr. P. Picouet
IRTA
Granja Comps 1 Armet, E-17121 Monells, Girona (Spain)

Dr. S. Yunus
Unite de Physice-Chimie et de Physique de Materieux
1. Pl. Croix du Sud, B-1348, Louvaine-La-Neuve (Belgium)

Dr. J.-E. Communal, Dr. F. Cordella, Dr. F. Quochi, Prof. A. Mura, Prof. G. Bongiovanni
Dipartimento di Fisica and Istituto Nazionale di Fisica della Materia
Università degli Studi di Cagliari
I-09042 Monserrato (CA) (Italy)

Prof. G. Di Silvestro
Dipartimento di Chimica Organica e Industriale, Università di Milano
via Venezian 21, I-20133 Milano (Italy)

[**] This work was partially supported by the EC RTN "Nanochannel" contract HPRN-CT-2002-00323 and the MIUR Progetto di Ricerca di Base Autonomo FIRB RBAU01N449.

tion imposed by the host, give very efficient Förster-type ET among the guest molecules, with emission from the lower-energy-gap molecule, even when its relative concentration is below 1 %.[6] The main advantages of these co-inclusion compounds are i) increased chemical stability of the active molecules, ii) emission with negligible self-absorption effects, and iii) efficient light conversion. The PHTP co-IC of several types of dyes can be suitably exploited to realize transport of energy and efficient down-conversion of light. Indeed, inorganic zeolite host materials with three guests have been already prepared, showing fascinating directional-transport properties mimicking those occurring in natural photosynthetic reaction centers.[7]

In this communication, we describe the preparation and characterization of a new nanostructured, fully organic material, namely a crystalline PHTP co-IC that forms well-aligned parallel nanochannels in which three different emissive linear molecules are accommodated. The absorption and emission spectra of the three molecules were chosen so that a sequential resonance energy transfer $1 \rightarrow 2 \rightarrow 3$ from the highest-energy molecule *1* to the lowest-energy molecule *3* can occur. The energy-transfer mechanism governing the photophysics of two guests in PHTP has been extensively studied.[6] In the case of host–guest systems containing three molecules, the kinetics of ET is intrinsically more complex, since it involves a two-step ET process $1 \rightarrow 2 \rightarrow 3$, where molecule *2* acts as both acceptor and donor. In this communication, we investigate the energy transfer among the three molecules by continuous-wave (CW) and time-resolved spectroscopy. We observe a fast $1 \rightarrow 2$ energy transfer, with emission from the blue dye reaching nearly 100 % efficiency. The second energy-transfer step $2 \rightarrow 3$ is relatively slow, allowing for simultaneous emission from dyes *2* and *3*, with efficient light emission in a wide range of the visible spectrum.

Figure 1a shows the structures of a host–guest crystal, and the guest molecules *p*-terphenyl (P3), 1,6-diphenylhexatriene (DPH), and pentathiophene (T5). As can be seen, the dyes are accommodated into the parallel nanochannels of the PHTP–crystalline adducts,[2] which are separated by about 1.4 nm. PHTP host–guest materials were obtained in the form of polycrystalline powders by successively melting and cooling the components in a stoichiometric ratio.[8] In order to test the complete inclusion and synthesize the adduct in the correct experimental conditions, the van't Hoff and Prigogine equations for liquidus curves, as modified by Farina,[9] were used. When the PHTP adduct was formed, a channel-like structure was obtained with channels completely filled by the guest molecules.[8,9] The occurrence of liquid-phase separation was confirmed by the differential scanning calorimetry (DSC) curves and by the overall phase diagram. If liquid-phase separation is expected, a very low cooling rate is used in the DSC apparatus during sample preparation. PHTP host–guest materials can also be obtained as needle-shaped crystals by slow solution evaporation,[5,10] or as thin films by vacuum-deposition techniques.[11]

In Figure 1b we report the picture of PHTP host–guest crystals illuminated with ultraviolet (UV) light. The blue emission from the crystals containing P3/DPH and the yellow-greenish color of the crystal containing P3/DPH/T5 dyes show that the UV light is converted into visible light throughout the PHTP host–guest crystal.

In Figure 2 we show the optical properties of the host–guest materials for both the single molecule IC and for the two- and three-molecule co-IC. (The absorption spectrum of the two-molecule co-IC is not shown because it is very similar to the three-molecule spectrum.) As can be seen, the photolumines-

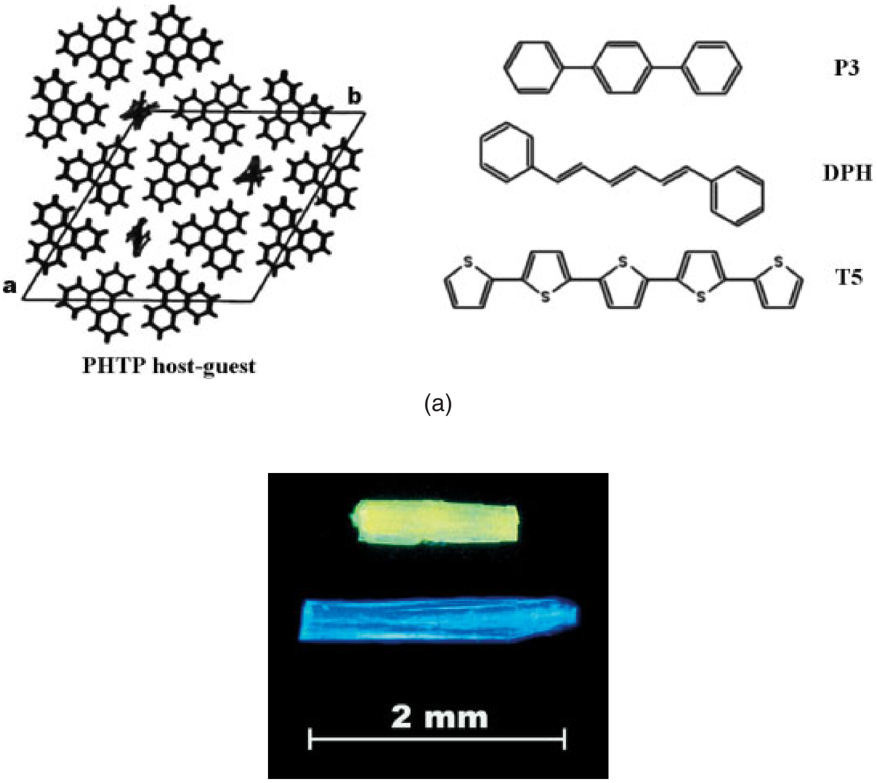

(b)

Figure 1. a) Left: Projection normal to the *c*-axis (with *a*- and *b*-axes labeled) of the pseudo-hexagonal unit cell of the guest-PHTP crystal, showing three nanochannels filled with guest molecules. Right: Molecular structure of the guest molecules *p*-terphenyl (P3), 1,6-diphenylhexatriene (DPH), and pentathiophene (T5). b) Optical microscopy image under UV-light illumination of host–guest crystals: P3/DPH–PHTP (molar ratio 80:20) crystal (bottom); P3/DPH/T5–PHTP (molar ratio 98.3:1.1:0.6) crystal (top). For the crystals, a 94:6 PHTP/guest molar ratio is obtained.

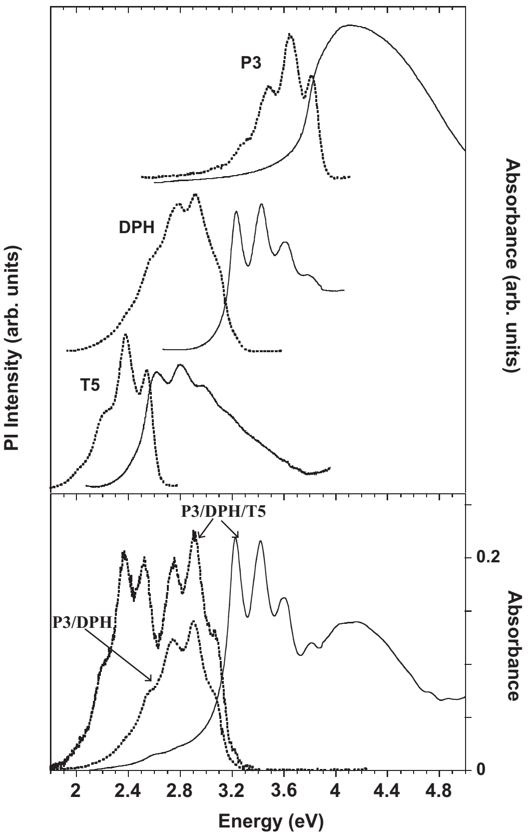

Figure 2. Room-temperature optical absorption (solid line) and photoluminescence (dotted line) spectra. Upper panel: P3, DPH, and T5 PHTP IC excited at the absorption maximum of each spectrum. Lower panel: PHTP co-IC two-molecule P3/DPH (molar ratio 56:44), and three-molecule P3/DPH/T5 (molar ratio 57:38:5) ICs. PHTP co-IC excited at 4.1 eV (P3 excitation). The spectra are normalized to similar intensities, and vertically shifted for clarity.

cence (PL) of P3 in the near-UV region overlaps well with the absorption of DPH. Moreover, a complete spectral overlap occurs between the PL of DPH, in the blue visible region, and the absorption of T5. This satisfies the condition for energy transfer from P3 to DPH, and from DPH to T5. In fact, resonance energy transfer from a donor (D) to an acceptor (A) occurs, with the same probability of the decay of the excited donor in the absence of acceptor, when the D–A distance is equal to the Förster radius R_0, defined as:[12]

$$(R_0)^6 \approx \frac{\eta_D \Gamma^2}{n^4} \int_0^\infty \frac{F_D(\omega)\varepsilon_A(\omega)}{\omega^4} d\omega \tag{1}$$

where η_D is the PL quantum yield of the donor in the absence of the acceptor, n is the refractive index of the medium, Γ^2 describes the relative spatial orientation of the transition dipoles of the donor and acceptor, the integral represents the spectral overlap between the (normalized) emission spectrum $F_D(\omega)$ of the D species and the extinction coefficient $\varepsilon_A(\omega)$ of the A species. The transfer rate k_{DA} from the donor to the acceptor increases strongly when the D–A distance R is smaller than the Förster radius R_0, according to the relation:

$$k_{DA} = \frac{1}{\tau_D}\left(\frac{R_0}{R}\right)^6 \tag{2}$$

where τ_D is the lifetime of the donor in the absence of the acceptor. By assuming a random distribution of parallel dyes ($\Gamma^2 = 0.593$),[13] according to Equation 1 average Förster radii $R_0 = 39$ Å and $R_0 = 44$ Å are obtained for the P3–DPH and the DPH–T5 ET, respectively. These values are compatible with efficient intra- and interchannel ET occurring between the included molecules. The partial superposition of DPH absorption and emission leads to an average Förster radius of about 29 Å for DPH–DPH transfers.

In the bottom of Figure 2, the optical properties of the co-IC of P3 and DPH are reported, showing only DPH emission during excitation of the P3 molecule. DPH excitation at 3.4 eV with light polarized along the *c*-axis resulted in PL-polarization ratios—measured as the ratio between the PL intensity polarized parallel and orthogonal to the *c*-axis—of about 5 for both DPH and P3/DPH host–guest crystals. These measurements indicate that a high degree of molecular orientation is attained by inclusion of the molecules in the PHTP crystal. The optical properties of the three-molecule co-IC material are also shown in the bottom of Figure 2. The absorption of the three-molecule co-IC material matches the P3 and DPH absorption, while the PL corresponds to the emission of both DPH and T5 when either P3 or DPH is excited.

In Table 1 the PL quantum yields (QYs) of the molecules in the host system are reported. The PL QYs are similar to those measured for the molecules dissolved in solutions: 0.82 and 0.32 for P3 and T5 in CH_2Cl_2 solution, respectively,[11,14] and 0.68 for DPH dissolved in ether. The QYs measured for DPH and T5 aggregate solid-state samples are much lower, less than 0.05.[11] These PHTP-based host–guest systems thus provide very efficient emitters in the solid state with high concentrations of active molecules. As for the co-IC, it is interesting to note that, by diluting the guest dye DPH within the higher-energy guest dye P3, the efficiency of DPH emission is in-

Table 1. PL quantum yields (QYs) of the molecules in PHTP. The QY values of co-inclusion compounds are averages taken for samples of different relative molar ratios, with an error of about 10 %. In parentheses, the molecules involved in the excitation/emission process are shown for the co-ICs.

Guest	Excitation [eV]	Emission [eV]	PL QY
P3	4.28	3.45–3.88	0.73
DPH	3.45	2.48–3.10	0.65
T5	2.95	2.07–2.58	0.31
P3/DPH	4.14–4.28 (P3)	2.48–3.10 (DPH)	0.74
P3/DPH	3.35–3.45 (DPH)	2.48–3.10 (DPH)	0.97
P3/DPH/T5	4.28 (P3)	2.07–3.10 (DPH+T5)	0.41
P3/DPH/T5	3.45 (DPH)	2.07–3.10 (DPH+T5)	0.66
P3/DPH/T5	2.95 (T5)	2.07–2.58 (T5)	0.37

creased compared to the inclusion of DPH alone. The lower PL QY of the P3/DPH/T5 co-IC compared with the two-molecule co-IC results from the low emission efficiency of the T5 molecule.

In Figure 3a, the PL decay of the DPH molecule is shown for the aggregate powder, the DPH IC, and the P3/DPH co-IC with two different molar ratios. The decay of the aggregate-powder sample is fast and non-exponential, in agreement with the fast migration of the photoexcitations towards non-radiative centers, which explains the extremely low PL QY. In the DPH IC and P3/DPH co-IC, the slower migration rate of the photoexcitations caused by the weaker intermolecular coupling[4] produces a longer PL-decay time and a higher QY. Figure 3a also shows that the PL-decay time increases with decreasing DPH concentration. This behavior is consistent with the fact that the higher-energy P3 molecules act as spacers. Even at a very low concentration of DPH, the PL lifetime (9 ns) compares favorably with those reported for the molecules dispersed in non-polar solvents[15] where the lower-energy excited state level is a 2^1 Ag state.[16]

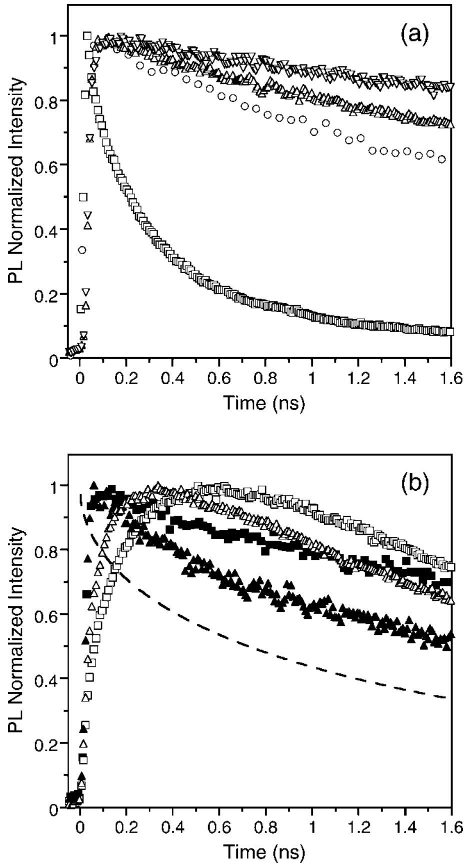

Figure 3. a) PL decay of DPH aggregate powder (squares), DPH–PHTP (circles), and P3/DPH–PHTP with relative molar concentrations of P3/DPH of 50:50 (triangles) and 99:1 (inverted triangles). b) PL decay of P3/DPH/T5–PHTP at P3/DPH/T5 relative molar concentrations of 45:42:13 (triangles) and 90:9:1 (squares), measured in the energy range 2.70–2.95 eV of the DPH emission (solid symbols), and in the energy range 2.10–2.30 eV of the T5 emission (open symbols). The theoretical DPH decay according to Equation 3, for a 1 % concentration of T5, is shown as a dashed line. The samples were excited at 3.26 eV (DPH excitation) at room temperature.

In the three-molecule co-IC, selective excitation of DPH allowed us to investigate the kinetics of the DPH–T5 energy transfer. In Figure 3b, the PL transients corresponding to emission energies of 2.22 eV and 2.81 eV are shown for two samples with different concentrations. The T5 spontaneous emission mainly contributes to the transient at 2.2 eV, while DPH represents the main contribution to the PL emission at 2.81 eV. Thus, the transients at the two emission energies can be used to monitor the excited state population of the T5 and DPH dyes. T5 emission rises rapidly, due to ET from DPH, increasing from 0 to 63 % (1 – 1/e) of its maximum value in 50–100 ps. The T5 rise time is longer in the samples with lower T5/P3 and T5/DPH ratios, due to the larger mean distance between DPH and T5. The PL decay of DPH is not exponential, and the initial decay time is fairly consistent with the rise time of T5. The correlation between the DPH–T5 mean distance and the DPH–T5 ET rate is corroborated by the quantitative analysis: the DPH decay time changes from 9 ns, to 5 ns, to 3 ns[17] with decreasing DPH–T5 mean distance in the P3/DPH/T5 samples with relative P3/DPH/T5 molar ratios of 99:1:0, 90:9:1, and 45:42:13, respectively. Finally, as the DPH–T5 ET is relatively slow, the T5 PL lifetime (~ 3 ns) is much longer than in solution (880 ps)[14] since the T5-population decay is compensated by the ET from the long-lived DPH species.

If the dye molecules are randomly distributed inside the nanochannels (i.e., the probability that a donor and an acceptor molecule occupy a crystal site is proportional only to the dye concentration), then the decay of the DPH photoluminescence I_{DPH} is described by:[6,18]

$$I_{\mathrm{DPH}}(t) \propto \mathrm{e}^{-t/\tau_{\mathrm{D}} - N_{\mathrm{F}}\sqrt{\pi t/\tau_{\mathrm{D}}}} \qquad (3)$$

where N_{F} is the mean number of acceptors within a sphere with the Förster radius. The non-exponential decay reflects the statistical distribution of the D–A distances. As time elapses, ET takes place between donor and acceptor sites separated by longer and longer distances, yielding a slower and slower decay.

Figure 3b shows the PL decay of DPH according to Equation 3 for a T5 concentration of 1 %. Equation 3 clearly overestimates the initial decay rate of the DPH PL. Since the early stage of the transfer dynamics theoretically is dominated by ET between nearest DPH–T5 pairs, the experimental data suggest that the probability of finding DPH and T5 at short distances is smaller than that predicted by a random, uncorrelated distribution of the dyes. We thus argue that, for these co-ICs, the low affinity between the T5 and DPH molecules enhances the probability of forming nearby D–D or A–A intrachannel pairs at the expense of D–A pairs. The low affinity between DPH and T5 favors the formation of donor-rich and acceptor-rich crystal phases on a microscopic scale. Deviation from a random distribution implies slower ET from DPH to

T5, and thus a higher ratio of T5 to DPH is necessary to obtain a broader spectral emission. From a materials-science perspective, this could represent an advantage, since higher T5 concentrations are easier to control.

In conclusion, we have prepared a new self-assembled fully organic host–guest system, where two and three emissive molecules are accommodated in the parallel nanochannels of a PHTP crystalline adduct. The emission from these materials is very efficient, since quenching effects typical of the solid-state phase are avoided. In the two-molecule system, we observe fast and efficient $1\rightarrow 2$ energy transfer, with emission from a blue emitter reaching 100 % efficiency for an optimal dilution of the emissive molecule *2* with the higher-energy molecule *1*. This material provides a perfect converter of light from ultraviolet to visible. By adding a lower-energy molecule *3* emitting in the green-orange region, we have realized a new host–guest material where a two-step resonance energy transfer $1\rightarrow 2\rightarrow 3$ occurs. Analysis of the energy transfer mechanism occurring in the three-molecule system shows that the $2\rightarrow 3$ energy transfer is slower than the $1\rightarrow 2$ transfer, due to the larger mean distance between the *2* and *3* molecules. However, thanks to the long lifetime of the blue-light-emitting *2* species, the slow $2\rightarrow 3$ energy transfer populates the green–orange-light-emitting *3* species, extending the emission through nearly the whole visible region and maintaining good emission efficiencies of 60–70 %. The use of this class of all-organic self-assembled nanostructured materials opens interesting perspectives for optoelectronic applications, as they provide highly efficient and tunable light converters for light-emitting diodes, and light-harvesting systems for photodetectors and solar cells.

Experimental

The guest molecules *p*-terphenyl (P3) and 1,6-diphenyl-1,3,5-hexatriene (DPH) were bought from Aldrich. Pentathiophene (T5) has been synthesized as reported in the literature [19] and purified using high-pressure liquid chromatography on a C18 stationary phase using CHCl$_3$ as eluent and a visible detector for T5. Perhydrotriphenylene (PHTP) was synthesized as reported in the literature [20]. Powders of inclusion and co-inclusion compounds were prepared by melting and successively cooling a mixture of guest molecules and PHTP in a Mettler 820 differential scanning calorimetry apparatus under a nitrogen atmosphere at a cooling rate of 0.1 K min^{-1} [8,9]. Crystals were obtained on a crystallization dish by slow evaporation of the compounds dissolved in distilled methyl ethyl ketone (MEK) at room temperature and under a N$_2$ flow. Crystals were washed with cold MEK. An excess of PHTP was used in all sample preparations to avoid any dye-aggregation effect. The relative molar ratios of dyes in the co-inclusion compound were determined by optical measurements in solution. Extinction coefficients of 33 800 M^{-1}cm^{-1} for P3 at 276 nm and 84 800 M^{-1}cm^{-1} for DPH at 353 nm in cyclohexane [21], and of 42 650 M^{-1}cm^{-1} for T5 at 417 nm in dioxane [22] were taken from the literature. Photoluminescence (PL) quantum yields (QYs) in solution was measured using quinine sulfate as a reference.

Optical absorption measurements were performed using a Perkin–Elmer Lambda-9 spectrometer on powders dispersed in KBr pellets. PL continuous-wave (CW) measurements were obtained with a SPEX 270 M monochromator equipped with a N$_2$ cooled charge-coupled device, and excitation with a monochromated Xe lamp. The optical spectra shown in Figure 2 were obtained on KBr pellets of IC with absorbances below 0.15 for PL measurements (in order to avoid re-absorption effects) and about 0.5–1.4 for absorption measurements. PL QYs on solids were measured using a home-made integrating sphere following the procedure reported in [23], and a monochromated Xe lamp. Values reported in Table 1 are averages for samples having different absorbances (powders, crystals or pellets of KBr dispersed powders), with an error of about 10 %. The PL QYs of co-ICs are reported as averages for samples of different relative molar ratios. The optical anisotropy of the crystals was determined by PL CW measurements made by exciting with the light polarized parallel or orthogonal to the needle axis (*c*), and analyzing the light with a polarizer filter in a backscattering geometry. PL polarizations are reported as the ratio between the intensity measured with the analyzer parallel and orthogonal to the needle axis (*c*-axis) when the exciting light is parallel to the *c*-axis. The reported values of PL polarization are averages obtained for different crystals, with variations of about 10 %.

The time resolved photoluminescence set-up consisted of a frequency-doubled femtosecond Ti:sapphire laser (Spectra Physics, Tsunami) and a streak camera (Hamamatsu, C5680). In order to obtain both time and spectral resolution, the streak camera was coupled to an imaging monochromator. The samples were excited at 3.27 eV by 100 fs pulses with a repetition rate of 80 MHz. In order to prevent heating, bimolecular recombination, and sample degradation, the average excitation power on the samples was maintained at 1 μW over a ~100 μm diameter spot. The fluorescence collected from the samples and focused on the entrance slit of the streak camera spectrometer was filtered below 420 nm to remove the remaining laser excitation. The time resolution of 3 ps of this setup was verified using the femtosecond laser pulse. The time-resolved fluorescence was measured from 1.91 to 3.10 eV simultaneously, and later integrated over the energy range of interest.

Received: February 12, 2004
Final version: June 9, 2004

---

[1] G. Calzaferri, S. Huber, H. Maas, C. Minkowski, *Angew. Chem. Int. Ed.* **2003**, *42*, 3732.
[2] R. Bosisio, C. Botta, A. Colombo, S. Destri, W. Porzio, E. Grilli, R. Tubino, G. Bongiovanni, A. Mura, G. Di Silvestro, *Synth. Met.* **1997**, *87*, 23.
[3] J. Cornil, D. Beljonne, D. A. Dos Santos, J. P. Calbert, J.-L. Brédas, *Thin Solid Films* **2000**, *363*, 72.
[4] G. Bongiovanni, C. Botta, J.-L. Brédas, J. Cornil, D. R. Ferro, A. Mura, A. Piaggi, R. Tubino, *Chem. Phys. Lett.* **1997**, *278*, 146.
[5] J. Gierschner, L. Lüer, D. Oelkrug, E. Musluoglu, B. Behnisch, M. Hanack, *Adv. Mater.* **2000**, *12*, 757.
[6] G. Bongiovanni, C. Botta, G. Di Silvestro, M. A. Loi, A. Mura, R. Tubino, *Chem. Phys. Lett.* **2001**, *345*, 386.
[7] M. Pauchard, A. Devaux, G. Calzaferri, *Chem. Eur. J.* **2000**, *6*, 3456.
[8] C. Botta, R. D. Ferro, G. Di Silvestro, R. Tubino, in *Supramolecular Photosensitive and Electroactive Materials*, (Ed: H. S. Nalwa), Academic, San Diego, CA **2001**, Ch. 5.
[9] M. Farina, G. Di Silvestro, *J. Chem. Soc., Perkin Trans. 2* **1980**, 1406.
[10] A. Quintel, J. Hulliger, *Synth. Met.* **1999**, *107*, 183.
[11] C. Botta, S. Destri, M. Pasini, P. Picouet, G. Bongiovanni, A. Mura, M. Uslenghi, G. Di Silvestro, R. Tubino, *Synth. Met.* **2003**, *139*, 791.
[12] a) J. R. Lakowicz, *Principles of Fluorescence Spectroscopy*, 2nd ed., Kluwer Academic/Plenum, New York **1999**. b) S. Speiser, *Chem. Rev.* **1996**, *96*, 1953.
[13] M. Z. Maksimov, I. M. Rozman, *Opt. Spectrosc.* **1962**, *12*, 337.
[14] D. Oelkrug, H.-J. Egelhaaf, J. Gierschner, A. Tompert, *Synth. Met.* **1996**, *76*, 249.
[15] E. D. Cehelnik, R. B. Cundall, J. R. Lockwood, T. F. Palmer, *J. Phys. Chem.* **1975**, *79*, 1369.
[16] B. E. Kohler, T. Itoh, *J. Phys. Chem.* **1988**, *92*, 5120.

[17] The decay times have been obtained by curve fitting the PL traces of DPH with a single exponential.
[18] B. Wieb van ver Meer, G. Coker III, S.-Y. Simon Chen, *Resonance Energy Transfer, Theory and Data*, Wiley, New York **1994**.
[19] S. Tasaka, H. E. Katz, R. S. Hutton, J. Orenstein, G. H. Fredrikson, T. T. Wang, *Synth. Met.* **1986**, *16*, 17.
[20] G. Allegra, M. Farina, A. Immirzi, A. Colombo, U. Rossi, R. Broggi, G. Natta, *J. Chem. Soc. B* **1967**, 1020.
[21] H. Du, R. A. Fuh, J. Li, A. Corkan, J. S. Lindsey, *Photochem. Photobiol.* **1998**, *68*, 141.
[22] R. S. Becker, J. S. de Melo, A. L. Maçanita, F. Elisei, *J. Phys. Chem.* **1996**, *100*, 18 683.
[23] J. C. de Mello, H. F. Wittmann, R. H. Friend, *Adv. Mater.* **1997**, *9*, 230.

Formation of Shell-Shaped Carbon Nanoparticles Above a Critical Laser Power in Irradiated Acetylene**

By *Mansoo Choi*,* *Igor S. Altman*, *Young-Jeong Kim*, *Peter V. Pikhitsa*, *Sanghoon Lee*, *Gyeong-Su Park*, *Taewon Jeong*, and *Ji-Beom Yoo*

In the last two decades, a series of novel nanostructured carbon materials have been synthesized in the laboratory,[1] including carbon nanotubes,[2] carbon onions,[3] and carbon nanocapsules.[4,5] Intensive studies of nanostructured carbon synthesis are motivated by potential applications such as intercalation materials for Li batteries,[6] gas-storage media, cold-electron field emitters,[7] etc. Consisting of bent graphene layers (GLs), these nanomaterials possess unique electric properties due to their finite characteristic size, making them attractive for such applications. Depending on the curvature of the graphene sheets, carbon nanomaterials can demonstrate metallic or semiconducting behavior.[8] As has been shown in our recent paper,[9] alternating metallic and semiconducting regions within carbon nanomaterials produces high levels of cold-electron field emission (FE) from nanostructured carbon materials. Therefore, there is a strong need to find an industrially attractive pathway to synthesize carbon nanoparticles with this structure.

It is worth noting that although a variety of methods have been developed to produce carbon nanomaterials, these methods generate only a raw product requiring either further purification (e.g., after laser ablation or arc discharge) or the removal of catalysts (after chemical vapor deposition). Herein, we report a new synthesis pathway for generating onion-like shell-shaped carbon nanoparticles (SCNPs) which is a one-step process. Our SCNPs are highly crystalline and not mixed with other types of carbon, and therefore do not need further purification. Furthermore, our method does not use any catalysts. We show that a transparent acetylene flow can produce onion-like SCNPs (which have continuous bent GLs) in bulk quantities when it is exposed to external irradiation from a continuous-wave (CW) infrared CO_2 laser. The striking feature of this process is that it is launched only above a critical threshold of laser irradiance. Below the irradiance threshold, the flame generates carbon soot. It is this critical threshold phenomenon that distinguishes our work from any other work in the field of flame-formed carbon nanoparticles. At the same time, we demonstrate that the formation of hollow SCNPs in our experiment has nothing to do with soot restructuring due to the ordering of basic structural units (BSUs), which has been recently reported in a hydrocarbon flame under pulsed irradiation from a Nd:YAG (YAG: yttrium aluminum garnet) laser.[10] The generation of SCNPs is governed by the direct growth of graphene sheets from precipitating acetylene molecules. The demonstration of the possibility of this latter process should be a significant contribution to the field of flame-formed carbon nanoparticles. We also show that our SCNPs exhibit FE performance comparable to that of carbon nanotubes.

Experiments have been carried out with the setup used successfully in our previous work.[11–15] The multi-nozzle-type burner allowed us to supply gases through different annular coaxial nozzles, permitting different types of gas flow. Pure acetylene (C_2H_2) was injected through the center nozzle within a stoichiometric co-flow oxyhydrogen flame, which provided acetylene heating.[16] Nitrogen flow between the outer oxyhydrogen flame and the inner acetylene flow prevented mixing of the gases. The flame was irradiated with a CO_2 laser beam. The vertical burner slide enabled us to change the irradiated flow position. The flame luminosity at the irradiated position was measured. The properties of the collected particles were examined by transmission electron microscopy (TEM), X-ray diffraction (XRD), Raman scattering, and magnetic measurements. The cold FE from SCNPs deposited onto a metal-coated (10 nm Cr and 100 nm Au) Si wafer was measured in a parallel-plate configuration within a vacuum chamber.[17]

---

[*] Prof. M. Choi, Dr. I. S. Altman, Y.-J. Kim, Dr. P. V. Pikhitsa,[+] S. Lee
National CRI Center for Nano Particle Control
Institute of Advanced Machinery and Design
School of Mechanical and Aerospace Engineering
Seoul National University
Seoul 151-742 (Korea)
E-mail: mchoi@plaza.snu.ac.kr

Dr. G.-S. Park, T. Jeong
Samsung Advanced Institute of Technology
P.O. Box 111, Suwon 440-600 (Korea)

Prof. J.-B. Yoo
Department of Materials Engineering
Sungkyunkwan University
Suwon 440-746 (Korea)

[+] Dr. P. V. Pikhitsa is on leave from the Physics Institute, Odessa National University, Odessa, Ukraine.

[**] This work was supported by the Creative Research Initiatives Program of the Ministry of Science and Technology, Korea. We thank Dr. J. M. Kim at Samsung Advanced Institute of Technology for field-emission measurements. Dr. I. S. Altman, Y.-S. Kim, Dr. P. V. Pikhitsa, and S. Lee contributed equally to this work.

DOI: 10.1002/adma.200400179